

Optical coatings grown by atomic layer deposition for high-power laser applications

Shin-ichi Zaitso^a, Shinji Motokoshi^b, Takahisa Jitsuno^a,
Masahiro Nakatsuka^a, and Tatsuhiko Yamanaka^a

^a Institute of Laser Engineering, Osaka University, 2-6 Yamada-oka, Suita, Osaka 565-0871, Japan;
zaitso@ile.osaka-u.ac.jp

^b Institute for Laser Technology, 2-6 Yamada-oka, Suita, Osaka 565-0871, Japan

Received 20 January 2003, in revised form 31 March 2003

Abstract. We prepared optical coatings with low (Al_2O_3) and high (TiO_2) refractive index materials using the sequential chemical reaction process of atomic layer deposition (ALD). Also, we examined the laser damage thresholds of the films for high-power laser applications. The highest damage thresholds were obtained for amorphous films grown at room temperature. For TiO_2 and Al_2O_3 films they equalled 5 and 5.2 J/cm², respectively. Finally, we employed ALD for growing desired refractive index coatings consisting of alternating nanoscale Al_2O_3 – TiO_2 laminated layers. The refractive index of the stack of these layers could be varied linearly from 1.61 to 2.39 by adjusting the thickness of the component layers.

Key words: atomic layer deposition, optical coating, laser-induced damage, refractive index.

1. INTRODUCTION

Atomic layer deposition (ALD) [¹] is one of the promising technologies to form atomic-scale controlled films with excellent physical quality. This technology makes it possible to control the film structure with atomic-layer level due to saturative nature of surface chemical reactions [^{1,2}]. Its unique features provide accurate and simple control of thickness, large-area thickness uniformity, excellent conformality, and good reproducibility. This method has been applied to highly conformal films [³], solar cells [⁴], and semiconductor processing of high-K dielectric films [^{5,6}].

Lasers for inertial confinement fusion (ICF) are equipped with a number of large-size optical components with multilayer coatings. These components require excellent performance depending on the error of thickness against design

values and uniformity over a large aperture (>300 mm), and laser-damage resistance. Conventional optical coatings are prepared by vacuum evaporation processes using a huge vacuum chamber and complicated mechanical operations (e.g. planetary rotating of substrates). In conventional methods, lack of controllability of thickness and large-area uniformity is one of the obstructions for construction of more advanced large-scale laser systems.

The outstanding characteristics of ALD as mentioned above may solve the problems accompanied with large evaporation coating systems, because the large-area uniformity and excellent controllability in ALD are suited to deposition of optical coating on large-size optical substrates with multilayer stacks. In addition, with ALD it will be possible to produce advanced components using its capability of atomic-layer tailoring of material composition in nanoscale levels.

In this paper, we summarize our works on optical coatings prepared by ALD for ICF laser application [7,8]. Especially we concentrate on laser-induced damage resistance and related properties for high-power laser applications. In addition, we show engineering of film properties (i.e. refractive index) by manipulating their composition in nanoscale levels. Our final purpose is fabrication of excellent optical coatings with high performance for high-power lasers and other advanced laser systems.

2. DEPOSITION PROCEDURE

In the ALD process, deposition of materials is achieved by chemical reactions of two different vapours dosed alternately into the growth chamber. The various procedures and chemical reactants for ALD of TiO₂ [9-15] and Al₂O₃ [16-20] have been used. In our experiments, we used tetrachlorotitanium (TiCl₄) and trimethylaluminium (Al(CH₃)₃) as cation sources for the growth of TiO₂ and Al₂O₃, respectively. Pure H₂O was used as an oxygen precursor. The vapours of the reactants were dosed into the evacuated chamber through timer-controlled electric valves. The position of the valves and the change of pressure in the chamber in one cycle are shown in Fig. 1. One cycle consisted of the dosing of TiCl₄, first evacuation, dosing of H₂O, and second evacuation. The vapours of TiCl₄ and H₂O were dosed into the chamber at a pressure of 10 mTorr and 100 mTorr, respectively. During the closing interval of the gate valve of 5 s, the vapours reacted with species on the surface of substrates. In order to prevent gas-phase reaction of these vapours, the gate valve was opened and the chamber was evacuated to a pressure below 10⁻⁴ Torr before another vapour was introduced. This cycle was repeated until the optical thickness reached a designed value. The thickness and the refractive index of films were measured by an ellipsometer (Gaertner Scientific Corporation) at a wavelength of 632.8 nm.

Laser damage thresholds were measured with a laser pulse of 1064 nm wavelength and a pulse width of 1 ns. The pulse generated from Q-switched Nd:YAG laser was focused onto the sample after two-stage amplification with

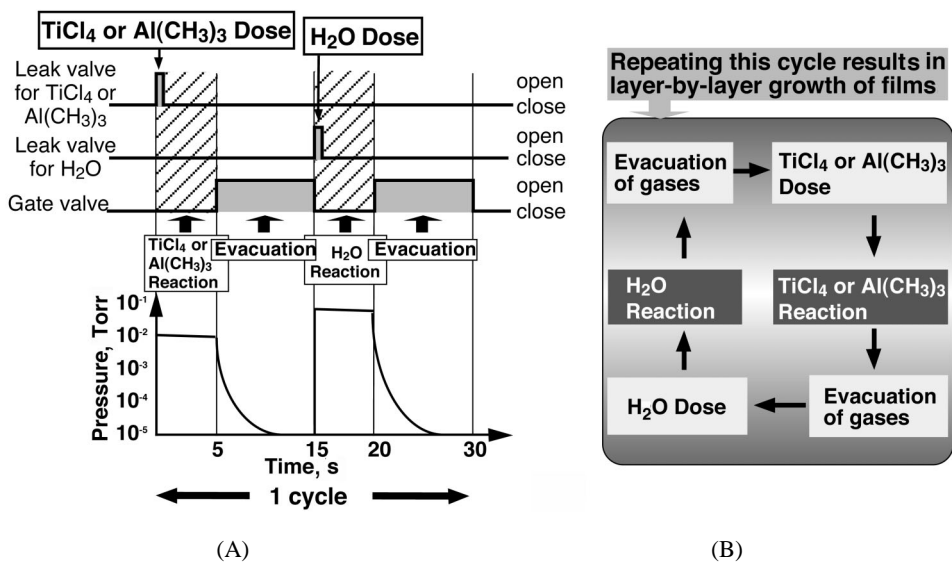


Fig. 1. (A) Position of each valve and the pressure in the growth chamber during one growth cycle. (B) Operations in one growth cycle.

Nd:YAG amplifiers. The laser beam had a smooth Gaussian spatial distribution with a spot diameter of 700 μm at $1/e^2$ peak intensity. We observed the irradiation site *in situ* with a microscope before and after each laser irradiation in order to detect laser-induced damage. The sample was moved after each laser shot, irrespective of the presence or absence of the damage. The laser damage threshold was defined as the smallest fluence at which any observable change occurred in the surface morphology of the irradiated area.

3. OPTICAL COATINGS FOR HIGH-POWER LASERS

Our growth chamber, equipped with a sample stage of 250 mm in diameter, can produce uniform thickness distribution over large-area substrates. Figure 2A,B shows thickness distribution of TiO₂ films on Si substrates arranged on the stage as described in Fig. 2C. The thickness variation was below 1% over an area of 240 mm in diameter. Flow directions of the reactant vapours and distance from dose nozzles had no influence on the deposition characteristics. This fact apparently results from uniform chemisorption of the reactant vapours during confinement steps in the deposition process and self-limiting nature of surface chemical reactions. This result indicates that our method was able to deposit films with high thickness uniformity by a simple procedure rather than complicated one in a large coating chamber, which is usually used in conventional evaporation processes. Our method, therefore, provides optical coatings for large-scale components, using a chamber that has barely sufficient

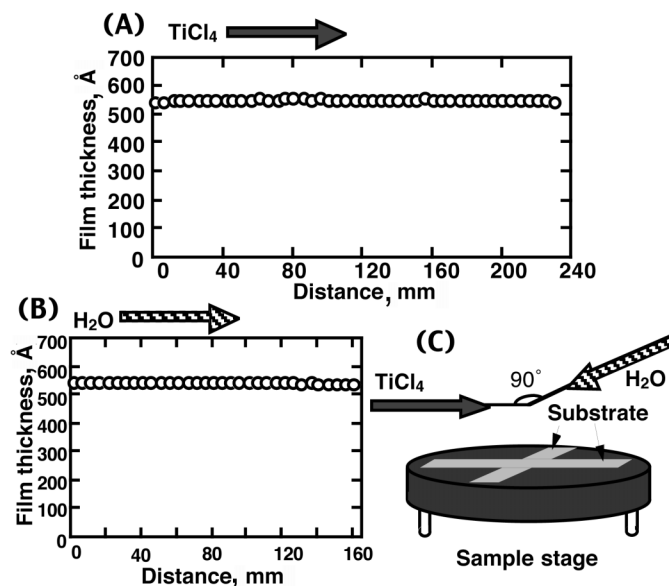


Fig. 2. Thickness distributions along the flow direction of TiCl₄ (A) and H₂O (B). The arrangement of Si substrate is shown in (C).

volume to contain the substrate. This fact will contribute to reducing the production cost for a high-power laser system such as an ICF driver.

Figure 3 shows the dependence of laser damage thresholds on the growth temperature. The largest value of Al₂O₃ films was 5.2 J/cm² and that of TiO₂ was 5 J/cm². The values were almost the same as those for films deposited by a conventional e-beam evaporation method in our laboratory (H. Yoshida and S. Motokoshi, unpublished results). The growth at low temperature provided the highest values of the laser damage threshold. The laser damage thresholds rapidly decreased as the growth temperature increased. In TiO₂ films, XRD measurements revealed that the decrease in laser damage thresholds was accompanied by crystallization of film materials with increasing growth temperature. This indicates that the crystalline structure of coating materials strongly affected the laser damage resistance of films. This fact can be explained by the increase in inhomogeneities in films due to the crystallization of materials. Therefore we expect that amorphous films grown at low temperatures are more suitable for high-power laser applications. On the other hand, Al₂O₃ films remained amorphous at these temperatures. We believe that the decrease in the laser damage resistance of Al₂O₃ films would result from the increase in packing density, which is generally observed in optical coatings deposited by various methods [21]. This explanation might be also adopted in the case of TiO₂ films. In addition to this effect, the laser damage resistance of TiO₂ was clearly influenced by its crystallization above the temperature of 250°C, because TiO₂ was substantially crystallized in this temperature range.

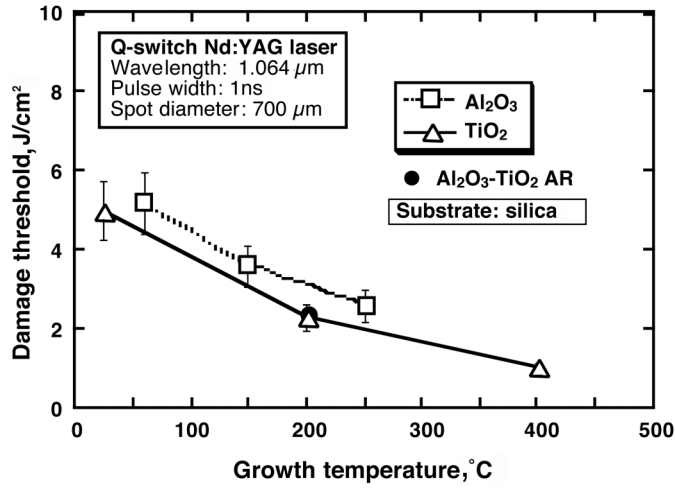


Fig. 3. Laser damage thresholds vs. growth temperature for TiO₂ and Al₂O₃ films with $\frac{1}{4}$ optical thickness on silica substrate.

4. CONTROL OF THE REFRACTIVE INDEX OF THIN FILMS

The growth rate per cycle in ALD is kept constant throughout the process, thereby ensuring that the film thickness increases linearly as a function of the number of cycles. In our experiment, the growth rates of Al₂O₃ ($g_{\text{Al}_2\text{O}_3}$) and TiO₂ (g_{TiO_2}) are 1.1 Å/cycle and 0.39 Å/cycle at the growth temperature of 200°C, respectively. Figure 4 shows a schematic of the alternately

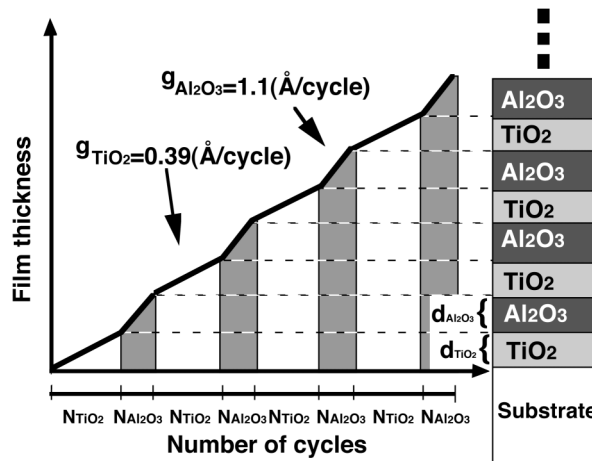


Fig. 4. Film thickness vs. the number of cycles, and the corresponding nanoscale structure with Al₂O₃-TiO₂ sublayers.

deposited nanoscale sublayers and the relationship between layer thickness ($d_{\text{Al}_2\text{O}_3}$ and d_{TiO_2}) and the number of growth cycles ($N_{\text{Al}_2\text{O}_3}$ and N_{TiO_2}). The thickness of a single sublayer of Al_2O_3 ($d_{\text{Al}_2\text{O}_3}$) and TiO_2 (d_{TiO_2}) can be expressed as follows:

$$d_{\text{Al}_2\text{O}_3} = g_{\text{Al}_2\text{O}_3} N_{\text{Al}_2\text{O}_3}, \quad (1)$$

$$d_{\text{TiO}_2} = g_{\text{TiO}_2} N_{\text{TiO}_2}, \quad (2)$$

respectively.

Al_2O_3 – TiO_2 bilayers were regularly stacked from the first bilayer to the last one. The volume concentration of Al_2O_3 of the coating is given by

$$C_{\text{Al}_2\text{O}_3} = \frac{d_{\text{Al}_2\text{O}_3}}{d_{\text{Al}_2\text{O}_3} + d_{\text{TiO}_2}}. \quad (3)$$

Using Eqs. (1) and (2), we obtain

$$C_{\text{Al}_2\text{O}_3} = \frac{1}{1 + g_{\text{TiO}_2} / g_{\text{Al}_2\text{O}_3} \times N_{\text{TiO}_2} / N_{\text{Al}_2\text{O}_3}}. \quad (4)$$

Since $g_{\text{Al}_2\text{O}_3}$ and g_{TiO_2} are constant in ALD, the volume concentration can be controlled by the ratio of the number of growth cycles of the two materials ($N_{\text{TiO}_2} / N_{\text{Al}_2\text{O}_3}$).

Figure 5 shows the dependence of the refractive index of the coatings on the volume concentration of Al_2O_3 . The indices were averaged because the nanoscale structure of the coating had a bilayer thickness much smaller than the wavelength. In Fig. 5, closed circles represent results when $N_{\text{Al}_2\text{O}_3}$ is fixed at 5 and N_{TiO_2} is varied from 5 to 100. It was found that the refractive index varied from 2.39 for pure TiO_2 to 1.61 for pure Al_2O_3 . The theoretical results obtained using the Drude and Lorentz-Lorenz formulas are also shown in Fig. 5. The dashed curve in Fig. 5 is the Drude model [22] assuming that the laser electrical field is parallel to the internal boundaries between different material layers. The solid curve is the Lorentz-Lorenz model [22] assuming that the film consists of the two randomly assigned materials with different polarizabilities. The experimental results agreed well with the Drude model (the dashed curve).

The conventional co-evaporation and co-sputtering methods are frequently used in the deposition of composite films. They need independent control of the relative deposition rates of the two evaporation sources or sputtering targets in order to control the composition of the film. Therefore, there have been many difficulties in the accurate control of the parameters. In our coating method, however, the ratio of the number of growth cycles of the two materials is the only parameter that affects the refractive index of the coating. This feature is a consequence of the accurate thickness controllability due to the self-limiting nature of the surface chemical reactions, which is unique to ALD.

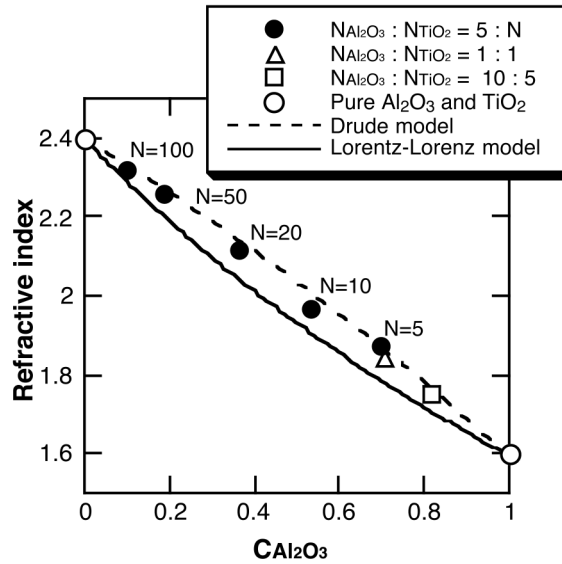


Fig. 5. Refractive index of films with alternating Al_2O_3 - TiO_2 sublayers vs. the volume concentration of Al_2O_3 .

In our model, we assumed that the growth rates were constant from the very initial cycles of the film growth. Other observation in ALD growth, however, showed the nucleation period in the early stage of the oxide growth and the deviation of the growth rate from the one of the enough thick (about a few nm) films [23]. In our experiments, the minimum thickness, which presents a linear growth property against the number of reaction cycles, is uncertain. We believe, however, that the control of the refractive index will be credible when using the sublayers with a thickness of a few nanometres because the excellent controllability of film thickness in ALD is incontestable in this region. In this connection, it might be more adequate that we should use experimentally measured values instead of the calculated $C_{\text{Al}_2\text{O}_3}$ as a horizontal axis in Fig. 5.

5. CONCLUSIONS

We prepared optical coatings with a low (Al_2O_3) and high (TiO_2) refractive index using the sequential chemical reaction process of ALD. The film thickness showed a proportional relationship to the number of operation cycles, and the error of film thickness distribution was less than 1% over an area of 240 mm in diameter. Furthermore, we examined the laser damage thresholds of the films for high-power laser applications. The highest damage thresholds of 5 J/cm^2 for TiO_2 films and 5.2 J/cm^2 for Al_2O_3 films were obtained for amorphous films grown at room temperature. Results from the analysis of the film structure and composition reveal that the decrease in laser damage thresholds as the growth

temperature rises is caused by the crystallization of the materials and the increase in packing density. Finally, we employed ALD for preparing desired refractive index coatings consisting of alternating stacks of nanoscale Al_2O_3 - TiO_2 laminated layers. The averaged refractive index of the whole stack assembly varied linearly from 1.61 to 2.39 by adjusting the thickness of sublayers.

REFERENCES

- Ritala, M. and Leskelä, M. Atomic layer deposition. In *Handbook of Thin Film Materials*, Vol. 1 (Nalwa, H. S., ed.). Academic Press, San Diego, 2002, 103–159.
- George, S. M., Ott, A. W. and Klaus, J. W. Surface chemistry for atomic layer growth. *J. Phys. Chem.*, 1996, **100**, 13121–13131.
- Ritala, M., Leskelä, M., Dekker, J. P., Mutsaers, C., Soininen, P. J. and Skarp, J. Perfectly conformal TiN and Al_2O_3 films deposited by atomic layer deposition. *Chem. Vapor. Depos.*, 1999, **5**, 7–9.
- Sang, B., Dairiki, K., Yamada, A. and Konagai, M. High-efficiency amorphous silicon solar cells with ZnO as front contact. *Jpn. J. Appl. Phys.*, 1999, **36**, 4983–4988.
- Kukli, K., Ihanus, J., Ritala, M. and Leskelä, M. Tailoring the dielectric properties of HfO_2 - Ta_2O_5 nanolaminates. *Appl. Phys. Lett.*, 1996, **68**, 3737–3739.
- Zhang, H., Solanki, R., Roberds, B., Bai, G. and Banerjee, I. High permittivity thin film nanolaminates. *J. Appl. Phys.*, 2000, **87**, 1921–1924.
- Zaitso, S., Motokoshi, S., Jitsuno, T., Nakatsuka, M. and Yamanaka, T. Large-area optical coatings with uniform thickness grown by surface chemical reactions for high-power laser applications. *Jpn. J. Appl. Phys.*, 2002, **41**, 160–165.
- Zaitso, S., Motokoshi, S., Jitsuno, T., Nakatsuka, M. and Yamanaka, T. Optical thin films consisting of nanoscale laminated layers. *Appl. Phys. Lett.*, 2002, **80**, 2442–2444.
- Ritala, M., Leskelä, M., Nylänen, E., Soininen, P. and Niinistö, L. Growth of titanium dioxide thin films by atomic layer epitaxy. *Thin Solid Films*, 1993, **225**, 288–295.
- Aarik, J., Aidla, A., Uustare, T. and Sammelselg, V. Morphology and structure of TiO_2 thin films grown by atomic layer deposition. *J. Cryst. Growth*, 1995, **148**, 268–275.
- Kumagai, H., Matsuoka, M., Toyoda, K., Obara, M. and Suzuki, M. Fabrication of titanium oxide thin films by controlled growth with sequential surface chemical reactions. *Thin Solid Films*, 1995, **263**, 47–53.
- Ritala, M., Leskelä, M., Niinistö, L. and Haussalo, P. Titanium isopropoxide as a precursor in atomic layer epitaxy of titanium dioxide thin films. *Chem. Mater.*, 1993, **5**, 1174–1181.
- Ritala, M., Leskelä, M. and Rauhala, E. Atomic layer epitaxy growth of titanium dioxide thin films from titanium ethoxide. *Chem. Mater.*, 1994, **6**, 556–561.
- Kukli, K., Ritala, M., Schuisky, M., Leskelä, M., Sajavaara, T., Keinonen, J., Uustare, T. and Härsta, A. Atomic layer deposition of titanium oxide from TiI_4 and H_2O_2 . *Chem. Vapor. Depos.*, 2000, **6**, 303–310.
- Schuisky, M., Aarik, J., Kukli, K., Aidla, A. and Härsta, A. Atomic layer deposition of thin films using O_2 as oxygen source. *Langmuir*, 2001, **17**, 5508–5512.
- Higashi, G. S. and Fleming, C. G. Sequential surface chemical reaction limited growth of high quality Al_2O_3 dielectrics. *Appl. Phys. Lett.*, 1989, **55**, 1963–1965.
- Fan, J., Sugioka, K. and Toyoda, K. Low-temperature growth of thin films of Al_2O_3 by sequential surface chemical reaction of trimethylaluminum and H_2O_2 . *Jpn. J. Appl. Phys.*, 1991, **30**, L1139–L1141.
- Ritala, M., Saloniemi, H., Leskelä, M., Prohaska, T., Friedbacher, G. and Grasserbauer, M. Studies on the morphology of Al_2O_3 thin films grown by atomic layer epitaxy. *Thin Solid Films*, 1996, **286**, 54–58.
- Kukli, K., Ritala, M., Leskelä, M. and Jokinen, J. Atomic layer epitaxy growth of aluminum oxide thin films from a novel $\text{Al}(\text{CH}_3)_2\text{Cl}$ precursor and H_2O . *J. Vac. Sci. Technol. A*, 1997, **15**, 2214–2218.

20. Ott, A. W., Klaus, J. W., Johnson, J. W. and George, S. M. Al₂O₃ thin film growth on Si(100) using binary reaction sequence chemistry. *Thin Solid Films*, 1997, **292**, 135–144.
21. Yoshida, K., Yaba, T., Yoshida, H. and Yamanaka, C. Mechanism of damage formation in antireflection coatings. *J. Appl. Phys.*, 1986, **60**, 1545–1546.
22. Aspnes, D. E. Optical properties of thin films. *Thin Solid Films*, 1982, **89**, 249–262.
23. Aarik, J., Karlis, J., Mändar, H., Uustare, T. and Sammelselg, V. Influence of structure development on atomic layer deposition of TiO₂ thin films. *Appl. Surf. Sci.*, 2001, **181**, 339–348.

Aatomkihtsadestamise meetodil kasvatatud optilised katted laseroptilisteks rakendusteks suuritel võimsustel

Shin-ichi Zaitso, Shinji Motokoshi, Takahisa Jitsuno, Masahiro Nakatsuka ja Tatsuhiko Yamanaka

Aatomkihtsadestamise meetodit kasutades on valmistatud väikese (Al₂O₃) ja suure (TiO₂) murdumisnäitajaga optilised katted. On uuritud kilede purunemislävesid suure võimsusega laserkiirguse korral. Suurimad läviväärtused, vastavalt 5 ja 5,2 J/cm², mõõdeti toatemperatuuril kasvatatud amorfsete TiO₂ ja Al₂O₃ kilede jaoks. Soovitud murdumisnäitajaga katete saamiseks valmistati nimetatud meetodil Al₂O₃-TiO₂ nanolaminaatkiled. Selliste komposiitkilede murdumisnäitajat oli võimalik komponentkilede paksusi varieerides muuta vahemikus 1,61–2,39.